

Deuterium retention in Tore Supra long discharges

E. Tsitrone, C. Brosset, J. Bucalossi, B. Pégourié, T. Loarer, P. Roubin², Y. Corre, A. Géraud, C. Grisolia, A. Grosman, J. Gunn, J. Hogan³, C. Martin², R. Mitteau, V. Philips⁴, D. Reiter⁴, J. Roth⁵, M. Rubel⁶, R. Schneider⁷, M. Warrier⁷

Association Euratom-CEA, CEA Cadarache, CEA-DSM-DRFC, F-13108 Saint Paul-lez-Durance, France

² : LPIIM, UMR 6633, Université de Provence, Centre Saint-Jérôme 13 397 Marseille cedex 20

³ : Fusion Energy Division, ORNL, Oak Ridge, TN 37831-8072 USA

⁴ : Institut für Plasmaphysik, FZ Jülich, Euratom Association, D-52425 Jülich, Germany

⁵ : Max Planck Institute für Plasmaphysik, Euratom Association, Boltzmannstr. 2, D-85748 Garching Germany

⁶ : Alfvén Laboratory, Royal Institute of Technology, Association Euratom VR, 100 44 Stockholm, Sweden

⁷ : Max Planck Institute für Plasmaphysik, Euratom Association, Teilinst. Greifswald, Wendelsteinstrasse 1, D-17491 Greifswald Germany

E-mail contact of main author : Emmanuelle.tsitrone@cea.fr

Abstract : Tritium retention is a crucial point to investigate for next step machines using carbon plasma facing components. In order to address this issue, particle balance has been performed on Tore Supra long discharges, allowing to estimate the wall deuterium inventory. In these conditions, large dynamic deuterium retention rates have been observed (up to 50% of the injected fuel). This paper presents a summary of the experimental results in terms of wall retention during the shot and particle recovery after the shot, as well as after glow discharges and disruptions. Particle balance integrated over a campaign is also estimated and compared with the D inventory deduced from sample analysis. Different mechanisms are then reviewed in order to explain this particle balance, from D particle implantation to carbon porosity filling and codeposition. Rough estimates of each process contribution to the retention rates are given and compared with the experimental observations.

1 Introduction

Tritium retention is a crucial point to investigate for next step machines using carbon plasma facing components. In order to address this issue, particle balance has been performed on Tore Supra long discharges, allowing to estimate the wall deuterium (D) inventory. This paper presents a summary of the experimental results obtained so far, and discusses proposed mechanisms to explain the large deuterium retention rates observed (up to 50% of the injected fuel). After a short summary of typical features of long pulses, section 2 presents the data obtained in terms of dynamic wall retention, particle recovery after the shot as well as after glow discharges and disruptions. The resulting global particle balance over a day of experiment or integrated over a campaign is then discussed and compared to the deuterium inventory estimated from sample analysis. Section 3 deals with the present understanding of the particle balance, and presents possible mechanisms to explain the experimental behaviour.

2 Experimental results

2.1 Long discharges scenarios and corresponding edge parameters

In typical long discharges scenarios [1], the plasma current is driven by lower hybrid (LH) power, which implies low density, low current plasmas. This results in high temperature low density plasma edge conditions ($n_e = 4 \cdot 10^{18} \text{ m}^{-3}$, $T_e = 100 \text{ eV}$ at the LCFS), quite different from the high density low temperature observed in typical divertor plasmas. The corresponding D^+ flux on the TPL is estimated to $\sim 10^{22} \text{ D/s}$ from reconstruction based on experimental data (see figure 2b in [2]). $T_i \sim 2T_e$ has to be assumed in the SOL in order to reproduce the heat load observed on the TPL.

Another specific feature of Tore Supra is that, due to the active cooling of the machine, the temperature of the plasma facing components is stationary a few seconds after the beginning

of the shot. For the main component in interaction with the plasma, the toroidal pump limiter (TPL), it lies in the range 120°C (temperature of the cooling loop) in the shadowed zones up to 350°C in the plasma loaded zones [3]. The carbon deposited layers in regions submitted to heat flux, like at the boundary between the shadowed/loaded zones on the TPL or on the neutralisers located below the TPL, can reach much higher temperature (up to 1000-1200 °C). The temperature excursion on the other plasma facing components, located further from the plasma, remains moderate (a few tens of degree above the cooling loop temperature).

2.2 Particle balance in long discharges

Figure 1 presents the time evolution of the wall retention rate as deduced from particle balance for 3 consecutive long discharges, separated by 30 minutes and 1 hour respectively. No conditioning procedure has been applied in between shots.

Two phases have been identified in the time behaviour of the wall retention rate. In the first phase (up to 100 s), it decreases (from $4 \times 10^{20} \text{ D s}^{-1}$ to $2 \times 10^{20} \text{ D s}^{-1}$), and in the second phase, remains constant throughout the pulse, with a typical value of $2 \times 10^{20} \text{ D s}^{-1}$, showing no sign of wall saturation even after more than 6 minutes of discharge. The wall inventory then becomes simply proportional to the pulse duration. The highest value reached so far is $7.8 \times 10^{22} \text{ D}$, out of which the excess trapped during the first phase (corresponding to the hatched area on Figure 1) is around 5×10^{21} . It is also seen that the shot to shot behaviour is identical, showing once again no sign of wall saturation even after 15 minutes of cumulated plasma time.

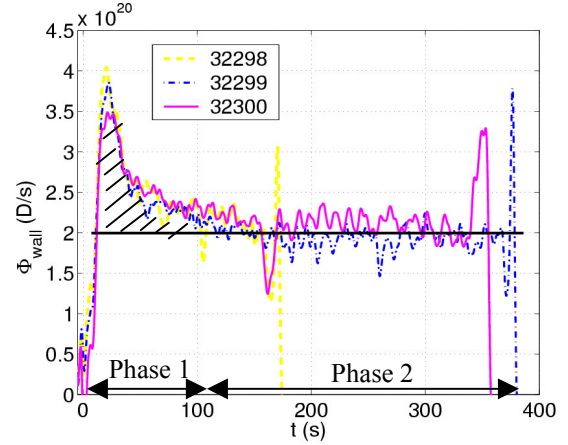


Figure 1 : wall retention rate calculated from particle balance during 3 consecutive long discharges

2.3 Particle recovery after shot

Particle recovery after the shot has been studied for a large database of discharges with LH power, including mainly long pulses but also a few shots at higher plasma current and density.

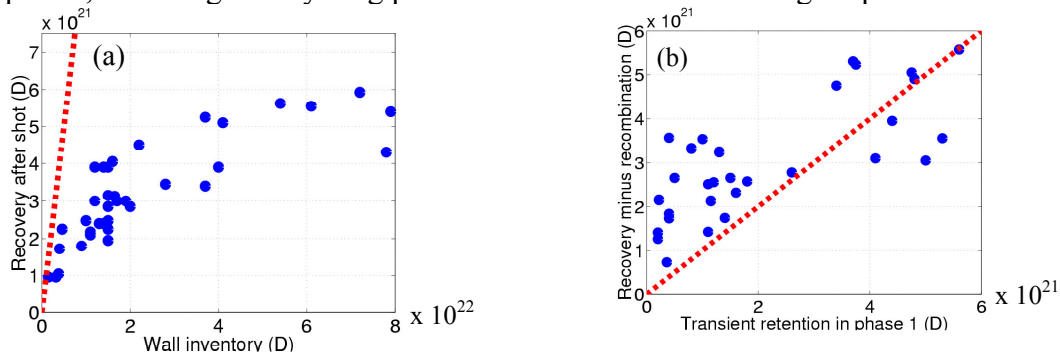


Figure 2 : (a) particle recovery after the shot as a function of the wall inventory reached at the end of the shot. The dashed line corresponds to a recovery equal to the wall retention. (b) particle recovery after the shot as a function of the estimated transient retention during phase 1. The plasma content at the end of the shot has been subtracted in order not to take into account the recombination of the plasma in the balance. The dashed line corresponds to a recovery equal to the transient retention

Figure 2 a) presents the particle recovery after shot as a function of the total wall inventory N_{wall} . It increases with N_{wall} for low wall inventory (ie for short discharges) and then stays constant around $5 \times 10^{21} \text{ D}$ for pulses longer than 2 minutes. In all cases, it is significantly

lower than the total wall inventory, from 60 % for the shortest discharges (~ 20 s) down to 5 % for the longest. It is also higher than the plasma content at the end of the discharge (3 to $5 \cdot 10^{20}$ D), which means than the wall outgases. This is coherent with a transient retention mechanism taking place during the first 100 s of the plasma, allowing particles to be recovered at the end of the shot.

In order to check this point, particle retention attributed to the transient retention mechanism during phase 1 N_{trans} (corresponding to the hatched area on Figure 1) has been estimated for the shots database. However, phase 1 is not always as clearly defined as is seen on Figure 1, specially for shots at higher plasma current and density, where it appears to be shorter (20s) and less marked, and sometimes simply not visible. However, N_{trans} has been computed for all the shots where it was possible (typically between 10 and 20 s on short discharges, 10 and 100 s on long discharges) and compared to the recovery after shot, from which the plasma content at the end of the discharge has been subtracted in order not to take into account the plasma recombination. Results are shown on Figure 2 b, where both quantities are seen to be correlated despite the large scatter of the data.

2.4 Particle recovery after glow discharge conditioning or disruptions

D₂ recovery by a night of He glow discharges has been monitored after several days of experiments with variable amounts of gas injected. The recovered inventory is about $30\text{-}40 \text{ Pam}^3$ ($1.5\text{-}2 \cdot 10^{22}$ D), independently of the quantity injected during the day (from 140 to 304 Pam^3). This is comparable to the estimated recovery of deuterium on 15 m^2 (total surface of carbon PFCs in Tore Supra) of saturated carbon on a depth corresponding to the incident energy of He (D concentration of 10^{21} D/m² for 20 nm of depth for 300 eV incident particles [4]). Most of the recovered deuterium is exhausted within the first 2 hours of the glow discharge.

As has been suggested in [5], disruptions can also lead to particle recovery, as is seen on Figure 3, where the total particle exhaust after a disruption is shown as a function of the plasma current I_p before the disruption, on a database of shots from the 2002 up to the 2004 campaign. The recovered quantities exhibit a threshold in plasma current as predicted in [5], since a threshold energy is needed to heat and outgas efficiently the D rich deposited layers. Below $I_p = 0.8$ MA, they are comparable to the usual recovery

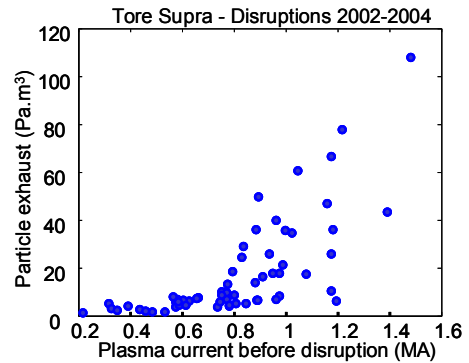


Figure 3 : Particle recovery after disruptions as a function of the plasma current before disruption

after shot ($5\text{-}10 \text{ Pam}^3$ or $2.5\text{-}5 \cdot 10^{21}$ D). They can reach up to $50\text{-}100 \text{ Pam}^3$ ($2.5\text{-}5 \cdot 10^{22}$ D if all the exhausted particles are assumed to be D₂) for the strongest disruptions at $I_p > 0.8$ MA. The IR imaging of the TPL, although too slow to catch the whole dynamic of the disruption (1 frame every 20 ms), has allowed to evidence heating of deposits which are usually located in the shadowed cold zones by the radiated energy dissipated by the disruption. This could be responsible for the large particle exhaust observed. However, a more detailed analysis is underway. In particular, the machine history (distance to the closest disruption, restart phase etc ...) could explain the large scatter in the data at a given I_p .

All the above numbers for wall loading and unloading are summarised in Table 1. In the following sections, these typical values will be used as guidelines in an attempt to identify the mechanisms responsible for the large experimental retention rates observed.

Wall loading for long discharges		Wall recovery		
<i>Phase 1 / transient</i>	<i>Phase 1 + 2 / permanent</i>	<i>Recovery after shot</i>	<i>Recovery after He glow discharge</i>	<i>Recovery after disruptions</i>
1-5 10^{21} D	10^{20} D/s x shot duration (up to $8 \cdot 10^{22}$ so far)	1-5 10^{21} D	1.5-2 10^{22} D	Up to $5 \cdot 10^{22}$ D at high I_p

Table 1 : summary of wall loading for long discharges and wall recovery

2.5 Integrated particle balance and comparison with measurements of the deuterium inventory in the machine

Particle balance has been performed over a whole day [6]. After short experiments (~ 20 s), leading to a moderate cumulated plasma time (~ 500 s), the integrated wall inventory (50 Pam^3) remains comparable to particle removal by a night of He glow discharge. Therefore the overall balance day of experiment / night of glow discharge would be close to zero. On the other hand, after long shots (~ 100 s), the cumulative plasma time and the associated wall inventory is higher (1800 s) while the recovery between shots is equivalent, leading to a higher integrated wall loading at the end of the day (300 Pam^3). This can not be recovered by a night of glow discharge and leads to the building up of a permanent wall inventory.

Based on the above day averaged net retention rates ($\sim 5 \cdot 10^{19}$ D/s for short discharges, $\sim 10^{20}$ D/s for long discharges), rough estimates of the D inventory build up integrated over a campaign can then be calculated, although it is highly uncertain to extrapolate. The total plasma cumulative time on the 2003-2004 campaign was $2.6 \cdot 10^4$ s, including ~ 4600 s of long discharges. This leads to a total D inventory of $1.5 \cdot 10^{24}$. Taking into account 30 nights of glow discharges ($4 \cdot 10^{23}$ D) and roughly 650 Pam^3 ($3 \cdot 10^{23}$ D) removed by disruptions, one ends up with a total D inventory of $8 \cdot 10^{23}$ D.

This can then be compared with experimental estimates of the D inventory in Tore Supra. Indeed, measurements of the D content in deposited layers sampled at different locations in the machine have been performed [7]. Two types of behaviour have been evidenced, as already found on other machines [8]. In “hot” deposited layers (D/C $\sim 1\%$), the D content is mainly concentrated in the first micron, while in the “cold” deposited layers in shadowed zones, the D/C ratio ($\sim 10\%$) stays constant over several μm s, so that the depth of the deposited layer has to be taken into account for D inventory calculations.

This method applied to samples analysed in [7] leads to a total inventory of $5 \cdot 10^{22}$ D, out of which 80 % is found in the cold deposits. However, a large fraction of the deposited layers present in the machine is still not analysed and not taken into account in this inventory, in particular on the surface of the TPL, which exhibit a complex pattern of deposits, mainly in gaps between tiles and at the boundary between plasma/shadowed area [6]. Rough estimates of the D content in these remaining layers, using the method described above, leads to an additional $\sim 4 \cdot 10^{22}$ D, yielding a total of $9 \cdot 10^{22}$ D present in the machine, still far below the estimated D inventory. However, large error bars on the two numbers prevents to draw any firm conclusion on the closing of the D balance in the machine, before the D content is accounted in non analysed carbon layers on the one hand, and an integrated particle balance is performed over a full experimental campaign on the other hand.

3 Present understanding of particle balance

As already stated, phase 1 could be interpreted as a transient retention process which saturates after ~ 100 s for typical long discharge conditions, combined to a permanent retention process. Phase 2 would correspond to the permanent retention process alone, once the transient process terminates. At the end of the shot, particles trapped by the transient retention process are then recovered. We now review possible mechanisms to explain the experimental observations.

3.1 Transient retention (phase 1)

Two mechanisms have been investigated in order to explain the decreasing retention rate during phase 1 : direct implantation of D particles in carbon plasma facing components, leading to a progressive saturation of the surfaces, and filling of porosity in the CFC, in particular in deposited layers.

3.1.1 Direct implantation of D in carbon

Direct implantation of D particles (D^+ ions and energetic charge exchange D_0 neutrals) has been estimated in [9]. The D^+ ions distribution is deduced from experimental measurements, while the D_0 distribution is computed with the Eirene code [10] in a simplified geometry set up (see [9] for details). Particle loading is then computed on the carbon plasma facing components. A simple model has been applied, based on particle implantation until a maximum D concentration in the carbon is reached. A complex pattern of particle implantation is evidenced, with saturation time constants ranging from less than a second to several hundreds seconds, compatible with the experimental behaviour during phase 1.

However, the above implantation modelling assumes to start from an empty carbon reservoir filled with deuterium during the shot, and does not explain the identical behaviour of successive discharges, unless a very strong diffusion takes place in the CFC material. For a diffusion coefficient $D_D = 10^{-19} \text{ m}^2 \text{ s}^{-1}$, which is probably an upper limit for the surface temperature of the plasma facing components [11] [4], this effect is moderate over the discharge duration and in between shots (the diffusion length in 1000 s would be 10 nm compared to typical implantation depth of 20 to 100 nm for D incident energy between 0.3 and 1 keV [4]). As a consequence, direct implantation of particles leads to the formation of a thin saturated layer (a few 10^3 's of nms) on all the plasma facing components, which is always present in normal operation (it can be depleted by disruptions and glow discharge conditioning), and does not play a role in the decreasing retention rate observed in phase 1.

3.1.2 Filling of porosity in the carbon material

Another mechanism could be the transient retention of D by adsorption in the porosity network of carbon, as is illustrated in Figure 4. The D particles, which diffuse in the transgranular macrovoids, can be adsorbed in the microvoids between crystallites, and then be released when the incoming flux is stopped (end of the discharge in our case). Porosity measurements have been performed on virgin CFC and on deposited layers sampled from Tore Supra neutralisers [12]. It was found that the neutralisers deposits have a 100 higher porosity than the virgin CFC. Absorption experiments were performed at 77 K at high pressure with different gases (CH_4 , N_2 , Ar ...). Extrapolation to H_2 leads to an absorption capacity of 10^{22} D/g of deposit. Extrapolation with temperature and pressure is more uncertain and could reduce this number by order of magnitudes. Experiments of absorption at room temperature are planned to clarify this point. In what follows, the upper limit of 10^{22} D/g of deposit is assumed, which leads to a quite moderate quantity of deposits (0.5 g or 0.625 cm^3) in order to account for typical inventories attributed to the transient retention in phase 1 ($5 \cdot 10^{21}$ D, see Table 1). High diffusion coefficient through pores ($D_{\text{pore}} \sim 10^{-12} \text{ m}^2 \text{ s}^{-1}$) have been reported, from theoretical work [13] as well as from experimental data [14]. This leads to possibly large diffusion length for particles into the pore network during the 100 s of phase 1, typically $10 \text{ }\mu\text{m}$. The surface of deposits needed to account for the D inventory (625 cm^2) is then small compared to the surface of deposits observed in the machine.

Moreover, outgassing after the pulse has also been analysed in order to check the consistency of particle release by the porosity network. Indeed, one expects the same time constant for filling and emptying the porosity network. The particle source S_{outgas} needed to reproduce the experimental behaviour of the vessel pressure p_{vessel} has been computed as follows :

$$dp_{\text{vessel}}/dt = S_{\text{outgas}} - S_{\text{eff}} P_{\text{vessel}}$$

where S_{eff} is the effective pumping speed of all the exhaust systems of Tore Supra. The computed source exhibits 2 times constants. The first peak corresponds to the plasma recombination, while the longer time constant ($\tau \sim 100$ s) would represent the porosity source, which is in good agreement with the typical duration of phase 1.

Therefore, filling of the porosity network in the deposited layers could be a good candidate to explain the retention rate attributed to transient retention during phase 1. However, the dependence of the adsorption with the surface temperature, the pressure and the nature of the incoming particles (ions/atoms/molecules) should be assessed. This is ongoing work.

3.2 Permanent retention (phase 1 and 2)

3.2.1 Codeposition

Codeposition of deuterium with carbon, whether it is due to carbon originating from physical erosion and leading to fresh layer growing and trapping deuterium, or sticking of hydrocarbons C_xD_y generated by chemical erosion and transported in shadowed areas, could lead to a constant retention rate as observed in phase 2. As a first check to this hypothesis, the carbon erosion source on the limiter has been estimated with the Eirene code used in the same setting as described in [9]. D_0 and D^+ have been considered. The erosion rates used are those given in [15], with the flux dependence turned off for the chemical sputtering erosion yield, which does not make a significant difference as all incident particle fluxes are below the threshold for this effect ($10^{22} \text{ m}^{-2}\text{s}^{-1}$). Adding the neutral and ions contributions leads to $2.35 \cdot 10^{20} \text{ C/s}$ and $1.5 \cdot 10^{20} \text{ CD}_4/\text{s}$. Self sputtering can also contribute significantly to the total erosion rates. It has been estimated in an independent calculation assuming 5% of C^{6+} in the incident flux on the TPL, which is coherent with the experimental $Z_{\text{eff}} = 2.5$ if the dominant impurity is carbon (considered here only as fully ionised C^{6+}). Adding all the contributions leads to a total erosion source of $6 \cdot 10^{20} \text{ C/s}$ and $1.5 \cdot 10^{20} \text{ CD}_4/\text{s}$. This source is likely to be underestimated as synergistic effect between ion and neutral bombardment has not been taken into account in the sputtering yield, nor the detailed surface temperature distribution (in particular the hot localised surfaces on the edge of the tiles and so on), which could act on the chemical erosion rates. However, it is roughly coherent with the supposed incoming C^{6+} flux if one assumes 90% of local redeposition on the TPL surface for instance. This leads to a moderate average net erosion on the TPL integrated over a campaign ($\sim 5 \mu\text{m}$), although of course the erosion pattern is not likely to be uniform as considered here. One can also check that the 10 % left for redeposition on other surfaces than the TPL (ie $6 \cdot 10^{19} \text{ C/s}$ and $1.5 \cdot 10^{19} \text{ CD}_4/\text{s}$) is consistent with the layer build up observed in the machine. For instance, the neutralisers layer ($800 \mu\text{m}$, growing rate 20 nm/s for 0.02 m^2) requires $3.8 \cdot 10^{19} \text{ C/s}$ while the layer in the shadowed zones of the TPL ($10 \mu\text{m}$, 0.25 nm/s for 0.3 m^2) requires $7.1 \cdot 10^{18} \text{ C/s}$. Therefore, the overall carbon balance is roughly coherent.

As far as the deuterium balance is concerned, the retention rate during phase 2 ($2 \cdot 10^{20} \text{ D/s}$) could be reached by assuming that 1/3 of the CD_4 created is transported and deposited in shadowed areas. Deposition of the above CD_4 rate integrated over the whole experimental campaign on the shadowed area of the limiter would lead to a thin layer of D rich carbon film. However, post mortem analysis of deposited layers in tokamaks exhibits a low D/C ratio (of the order of 10 % at most in general). On the other hand, if one supposes that D films are formed directly at the ratio $D/C = 0.1$ as observed, then a carbon influx of $2 \cdot 10^{21} \text{ C/s}$ is needed. This would require a much higher erosion source, which does not seem compatible with the experimental Z_{eff} and would lead to quite thick deposits (more than $100 \mu\text{m}$ on the 4 m^2 of the shadowed zone), which have not been observed in the machine. However, thick deposits in gaps between tiles, dust and flakes production, and deposited layers on other

surfaces than the limiter have been observed, so that the amount of deposited C present in the machine still needs to be more carefully accounted. Another possible explanation would be that D rich films are formed by codeposition in shadowed areas during the plasma phase, accounting for the dynamic D retention observed with a reasonable C deposition rate. These D rich films could subsequently be eroded and depleted in D (conditioning procedures, disruptions ...). A relatively thin C deposited layer could then be consistent with both a high dynamic retention during the plasma phase (high D/C ratio) and a lower long term retention as deduced from post mortem analysis (lower D/C ratio). Therefore, to the present stage of knowledge, although it can not be ruled out, it seems hard to explain the high retention rate observed during phase 2 with codeposition only. Modelling work with dedicated carbon erosion and transport codes is underway to better characterize this process.

3.2.2 Further mechanisms

Another highly speculative mechanism could be a diffusion through the pores of CFC, which would start once the open porosity at the surface of the material are saturated, and could then lead the deuterium into deeper layers of the carbon materials where it could be trapped. Indeed, recent theoretical description of hydrogen transport in carbon [16] has underlined the importance of an equivalent “molecular” diffusion (in fact a sequence of dissociation and recombination of the molecule diffusing in microvoids) to lead the H atoms to the traps on the surface of the crystallites (see Figure 4). In this work, the incident molecule is first diffusing into the macrovoids, then diffusing into the microvoids with an equivalent activation energy of 1.3 eV. It can then reach the edge surfaces of the crystallites where it can be trapped if trapping sites (called traps 2 in Figure 4) are still available. Once these sites are saturated, it

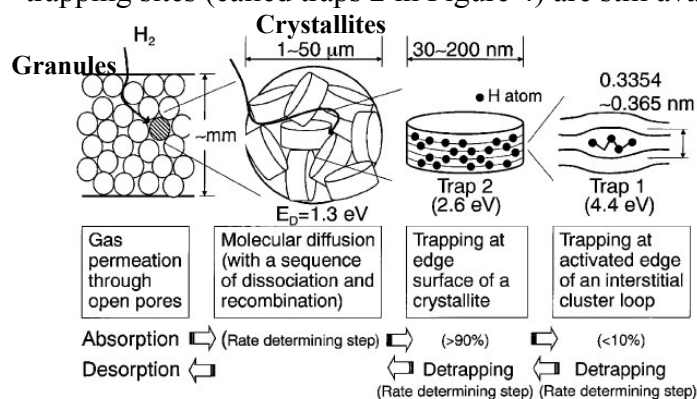


Figure 4 : schematic illustration of hydrogen transport and trapping in carbon as proposed in [16]

retention between short discharges (where this process is not triggered as the porosity are not filled) and long discharges, as has been evidenced in [17].

The experimental retention rate could then be understood as the contribution from 3 mechanisms : 1) filling of the surface porosity, which gradually stops when they are saturated, 2) diffusion through the pores which starts once the pressure is high enough and leads to trapping in deep layers, and 3) codeposition, which remains constant.

4 Summary and prospects

In Tore Supra long discharges, high retention rates have been observed (~50 % of the injected fuel), with a typical 2 phases behaviour. In the first phase (~100 s), it is seen to decrease before stabilising in a second phase to a constant value, showing no sign of saturation even after 6 minutes of discharge.

By analysing the recovery after shot (only a small fraction of the particles trapped during the discharge), it was found that the decreasing phase is probably associated with a transient

retention process while the constant rate would correspond to a permanent retention process. Recovery after a night of glow discharge or a disruption remains moderate compared to the wall inventories involved.

Several processes have been reviewed in order to explain the experimental retention rates. Implantation of D in carbon and progressive saturation of the interaction surfaces is probably not playing any role in the decrease of the retention rate observed in phase 1, as the implanted particles can not diffuse fast enough to empty the reservoir for the next shot. Progressively filling the open surface porosity of the carbon could be a candidate for the transient retention mechanism. Indeed, high porosity have been measured on deposited layers of Tore Supra. However, more work is needed to assess the adsorption capacity of the carbon in a tokamak environment (temperature, pressure, incident particles). Codeposition has been examined as a candidate for the permanent retention mechanism. Erosion sources coherent with the observed layer growth and the plasma impurity content have been estimated. However, they do not seem to be high enough to explain the observed D retention if the deposited layers have a D/C ratio of 10%, as measured in post mortem analysis of Tore Supra samples. Another highly speculative mechanisms could be a diffusion through the pores of CFC, which would start once the open porosity at the surface of the material are saturated, and could then lead the deuterium into deeper layers of the carbon materials where it could be trapped.

Refined modelling is now underway to better assess the contribution of the above mechanisms, in particular concerning carbon erosion and transport. Other experimental long pulses scenarios, involving higher power/density discharges, are now also being studied. With its ability to pursue long discharges with actively cooled components, Tore Supra offers a unique opportunity to distinguish between the different processes at stake in deuterium retention over time scales relevant to plasma wall interactions in next step machines.

References

- [1] : D. Van Houtte, G Martin, A Becoulet et al., Nucl. Fusion 44 (2004), L11-L15
- [2] : A. Grosman et al., 16th International Conference on Plasma Surface Interactions in Controlled Devices (PSI 2004, Portland, USA), to be published in J. Nucl. Mater.
- [3] : R. Mitteau et al., Physica Scripta, vol T111, 157-162 (2004)
- [4] : K. L. Wilson et al., in "Atomic and Plasma Material interaction data for fusion", Supplement to Nuclear Fusion, IAEA (1991) volume 1, p 31
- [5] : D. Whyte et al., 16th International Conference on Plasma Surface Interactions in Controlled Devices (PSI 2004, Portland, USA), to be published in J. Nucl. Mater.
- [6] : B. Pégourié et al., Physica Scripta, vol T111, 23-28 (2004)
- [7] : C. Brosset et al., 16th International Conference on Plasma Surface Interactions in Controlled Devices (PSI 2004, Portland, USA), to be published in J. Nucl. Mater.
- [8] : M. Rubel et al., Physica Scripta, vol T111, 112 (2004)
- [9] : E. Tsitrone et al., 16th International Conference on Plasma Surface Interactions in Controlled Devices (PSI 2004, Portland, USA), to be published in J. Nucl. Mater.
- [10] : see www.eirene.de
- [11] : R. A. Causey et al., J. Nucl. Mater., 300 (2002) 91-117
- [12] : P. Roubin et al. 16th International Conference on Plasma Surface Interactions in Controlled Devices (PSI 2004, Portland, USA), to be published in J. Nucl. Mater.
- [13] : M. Warrier et al., Contrib. Plasma Phys. 44, No. 1-3, 307-310 (2004)
- [14] : L. A. Sedano et al., J. Nucl. Mater., 258-263 (1998) 662-665
- [15] : J. Roth et al., J. Nucl. Mater., 266-269 (1999) 51-57
- [16] : H. Atsumi et al., J. Nucl. Mater., 313-316 (2003) 543-547
- [17] : T. Loarer et al., EX/P5-22, these proceedings